

Experimental studies of rubidium absolute polarization at high temperatures

S. Appelt,^{a)} T. Ünlü, K. Zilles, and N. J. Shah
Institut für Medizin, Forschungszentrum Jülich, 52425 Jülich, Germany

S. Baer-Lang and H. Halling
Zentrales Elektronik Labor, Forschungszentrum Jülich, 52425 Jülich, Germany

(Received 1 April 1999; accepted for publication 26 May 1999)

We report on measurements of the absolute rubidium (Rb) polarization, optically pumped by a high-power diode laser array, up to temperatures of 180 °C. The penetration of the pump laser light into a high-pressure cell has been studied experimentally and theoretically. The experimental results are compared to a model, which describes the local Rb polarization and optical pumping rate in the cell. © 1999 American Institute of Physics. [S0003-6951(99)03229-5]

In nuclear magnetic resonance and in other fields of science such as human MRI,¹⁻⁴ material and surface physics,^{5,6} the production of hyperpolarized noble gases through spin exchange with optically pumped alkali-metal atoms has gained importance. For some potential applications such as ¹²⁹Xe brain imaging,⁴ very high nuclear polarizations are required to circumvent the limitations of the delivery method⁷ and to avoid the anaesthetic effects of large quantities of Xe in the brain.

We have built a Rb-Xe hyperpolarizing unit, similar to that described by Driehuys *et al.*,⁸ for the production of several grams of polarized Xe ice. In order to optimize the Rb (and thus Xe) polarization, a low-cost and compact polarization imaging device was developed which enables measurement of the distribution of the absolute Rb polarization in the pumping cell. The methodology and first experimental results of absolute Rb polarization imaging in high-pressure optical pumping cells at a temperature of $T=100$ °C were recently published by Baranga *et al.*⁹ and Young *et al.*¹⁰ Spin exchange optical pumping at temperatures higher than 100 °C causes the spin exchange rate between Rb and Xe to be larger and therefore the time required to polarize Xe atoms is significantly shorter.

Experimental results of the absolute ⁸⁵Rb polarization in high pressure optical pumping cells for temperatures up to 180 °C are presented. The measured, volume-averaged absolute Rb polarization sets a limit on the maximum achievable Xe nuclear polarization at high temperatures. Furthermore, we studied the penetration of the pump laser light into the cell at a temperature range from 120–180 °C.

Figure 1 shows a schematic diagram of the compact, low-cost ⁸⁵Rb polarization imaging unit. For the sake of clarity, components of the Rb-Xe polarizer necessary for operating in a flowing mode and to freeze out the Xe gas are not shown. The optical pumping cell consisted of a glass cylinder with flat glass windows in order to avoid lens effects on the pump laser beam. The cell (inner diameter 24 mm, length 70 mm) was filled with approximately 1 g of Rb, 7 atm of ⁴He, and 0.07 atm of N₂ and Xe gas. For optical pumping parallel to the magnetic field B_0 (z axis), we use a fiberoptically coupled diode laser array (Opto Power Corp., OPC

100) with a maximum output power of 100 W and a line-width of 2 nm. The absolute ⁸⁵Rb polarization was measured by detecting, optically in the transverse mode, the Zeeman transitions of ⁸⁵Rb in a high magnetic field. The Zeeman spectrum was obtained by sweeping the magnetic field B_0 from 53.5 to 56.5 G and irradiating with an rf field of a few Watts of power and with a fixed frequency of 25 MHz. For optical detection, we used a single-mode laser diode (SONY SLD 203 AV, 20 mW) instead of a Ti: sapphire laser system. Compared to the Ti: sapphire laser, the laser diode is a low-cost device and has less intensity noise if a stable current and temperature controller are used. The compact laser diode module was mounted together with a mirror, a $\lambda/4$ plate, a lens, a photodetector, and a home-built G_x -gradient coil on a platform. This platform can move along the z axis of the pumping cell (see Fig. 1). In this way two-dimensional x - z slices of the ⁸⁵Rb absolute polarization were readily measured over a temperature range of 120–180 °C. At high Rb spin densities above 160 °C, the light of the 100 W pump laser cannot penetrate too far into the vapor and Rb-Rb spin exchange considerably broadens the Zeeman transitions.¹¹ Therefore, Rb polarization measurements are more difficult at higher temperatures. Following Walker and Happer,¹² the

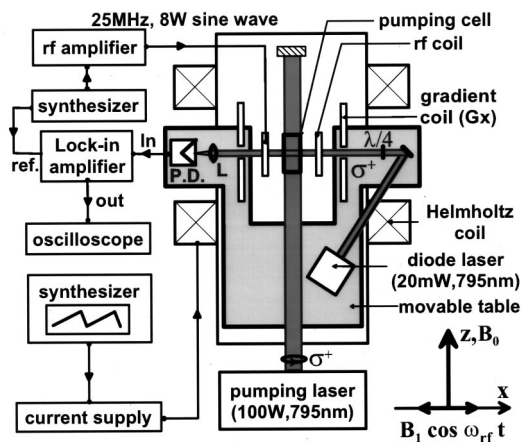


FIG. 1. Schematic diagram of the Rb imaging unit. The laser diode, photodetector, optical components, and gradient coil were mounted on a platform and moved together along the z direction. For the sake of clarity the oven and the components necessary to freeze out the Xe are not shown.

^{a)}Electronic mail: appelt@fz-juelich.de

penetration of the pump laser light into the cell can be calculated by solving the equation $dF/dz = -n_{\text{Rb}}(1-P)R$, which describes the attenuation of the photon flux F along the path z . dF/dz depends on the Rb number density n_{Rb} , the optical pumping rate R and the Rb polarization P , which is given for high pressure optical pumping cells as:^{9,11}

$$P = s_z \frac{R}{\gamma_{sd} + R}. \quad (1)$$

γ_{sd} is defined as the rate of spin destruction and s_z is the photon spin of the circularly polarized pumping laser. For a Gaussian laser profile with a width of $\delta\lambda_l$ the optical pumping rate R depends on the photon flux F in the following way:¹³

$$R = \frac{2\sqrt{\pi} \ln 2 r_e f \lambda_l^3 w'(r, s)}{hc \delta\lambda_l n_p} \frac{I_l n_p}{A} = 7.5 \times 10^{-15} \text{ cm}^2 F, \quad (2)$$

where r_e is the classical electron radius, I_l is the pump laser power, A is the effective area of illumination and $n_p = 4 \times 10^{18} \text{ J}^{-1}$ is the number of photons per Joule at the pump laser wavelength $\lambda_l = 800 \text{ nm}$. Note, that in Eq. (2) $F = I_l n_p / A$ and the factor $7.5 \times 10^{-15} \text{ cm}^2$ is calculated for our experimental conditions, namely $\delta\lambda_l = 2 \text{ nm}$, $f = 1/3$ (oscillator strength of Rb- D_1 -line) and for the real part of the complex overlap function $w'(r=0.135, s=0) = 0.885$. Together with Eqs. (1) and (2), the attenuation of the photon flux F can be written as a nonlinear differential equation for R as:

$$\frac{dR}{dz} = -\beta \left(1 - s_z \frac{R}{\gamma_{sd} + R} \right) R. \quad (3)$$

The parameter $\beta = 7.5 \times 10^{-15} \text{ cm}^2 n_{\text{Rb}}$ depends on the Rb-number density n_{Rb} and thus on the temperature of the cell.¹⁴ Equation (3) can be readily solved by separation of variables leading to an implicit solution for R such that

$$[1 + a(\beta z + K)]R + \gamma_{sd} \ln R + \gamma_{sd}(\beta z + K) = 0, \quad (4)$$

where $a = 1 - s_z$ and the constant K is determined by the boundary condition $R_{(z=0)} = R_0$. R_0 is the initial optical pumping rate at $z=0$. The boundary condition forces the constant K to be $K = -(R_0 + \gamma_{sd} \ln R_0) / (\gamma_{sd} + aR_0)$. Equation (4) represents the analytical model which will be compared to our experimental results. The functional form of Eq. (4) is determined by the four parameters s_z , γ_{sd} , R_0 , and n_{Rb} . We measured the photon spin of the pump laser $s_z = 0.96 \pm 0.02$ within a few percent error. Furthermore, we set $\gamma_{sd} = 21\,000 \text{ s}^{-1}$, a value which was calculated from the known value of the spin destruction $\gamma_{sd} = 30\,000 \text{ s}^{-1}$ for a cell containing 0.1 atm of Xe gas.⁹ R_0 was estimated for 100 W of laser power using Eq. (2) and knowing the approximate effective area $A \approx 13 \text{ cm}^2$, resulting in $R_0 \approx 240\,000 \text{ s}^{-1}$. Although we were unable to measure the precise Rb number density, because of the unavailability of a tunable probe laser, we obtained an approximate value of n_{Rb} by measuring the temperature close to the cell. At a nominal temperature of 180 °C, there was a negative temperature gradient of 10 °C from the front to the back of the cell. Additionally, the cylindrical pumping cell has an inlet and outlet where the temperature was also lower. Therefore, we expect, especially at high temperatures, where we measured the largest gradients,

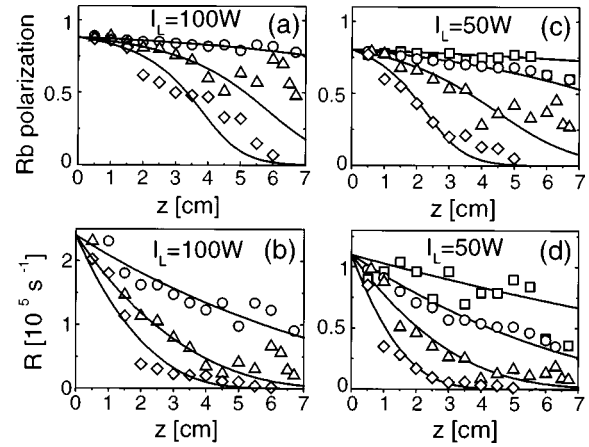


FIG. 2. Absolute Rb polarization P and optical pumping rate R as a function of the penetration depth z for 100 W (a),(b) and 50 W (c),(d) of pump laser power. The squares, circles, triangles, and diamonds correspond to measurements taken at 120, 140, 160, and 180 °C. The solid lines represent the theory given by Eq. (4) with the model parameters $s_z = 0.96$, $\gamma_{sd} = 21\,000 \text{ s}^{-1}$, $R_0 = 240\,000 \text{ s}^{-1}$ for 100 W ($110\,000 \text{ s}^{-1}$ for 50 W).

a reduced Rb number density. Figure 2 shows the experimental results of the absolute Rb polarization P [Figs. 2(a) and 2(c)] and the optical pumping rate R [Figs. 2(b) and 2(d)] as a function of the penetration depth, z , into the pumping cell. Because no gradient G_x was present during the measurements, each point in Fig. 2 represents an average polarization along the x axis of the detection beam. The local optical pumping rate $R_{(z)}$ is calculated from P using Eq. (1). Figures 2(a) and 2(b) show the polarization, P , and the optical pumping rate, R , for the pump laser power of 100 W and Figs. 2(c) and 2(d) correspond to measurements at 50 W, respectively. The absolute polarization was determined at four different temperatures (all measured in front of the cell), at $T = 120$ (squares), 140 (circles), 160 (triangles), and 180 °C (diamonds). The solid lines represent the model given by Eq. (4) and evaluated for $s_z = 0.96$, $\gamma_{sd} = 21\,000 \text{ s}^{-1}$, $R_0 = 240\,000 \text{ s}^{-1}$ for 100 W and $R_0 = 110\,000 \text{ s}^{-1}$ for 50 W. The Rb number densities n_{Rb} and thus the parameter β have been varied in order to fit to the experimental results. The resulting values for β are: $\beta = 0.438, 1.103, \text{ and } 1.7$ for 100 W and $\beta = 0.159, 0.438, 0.904, \text{ and } 1.782$ for 50 W. These correspond to temperatures of 139, 157, and 166 °C for 100 W and 121, 139, 153, and 167 °C for 50 W.¹⁴ The values of β resulting from the fit to our model yield temperatures which are in close agreement with the measured temperatures 120 and 140 °C at the front of the cell but deviate by 7–14 °C from the measured values at higher temperatures (160 and 180 °C). Note, that for high temperatures and for $z > 4 \text{ cm}$ the measured values for P are larger than those predicted by the model. All deviations at higher temperatures are probably due to temperature gradients which reduce n_{Rb} in the back of the cell. Nevertheless, up to 160 °C the model is in close agreement with the measured data. The volume-averaged Rb polarization $\langle P \rangle$ (in percent) was evaluated from the data in Fig. 2 for each temperature. For 100 W $\langle P \rangle = 84\%, 69\%, \text{ and } 47\%$ for $T = 140, 160, \text{ and } 180$ °C and $\langle P \rangle = 75\%, 70\%, 49\% \text{ and } 28\%$ for $T = 120, 140, 160, \text{ and } 180$ °C. We found that with time some Rb is transported from the Rb reservoir to the walls of the cell. After a few minutes of optical pumping with 100 W and at temperatures

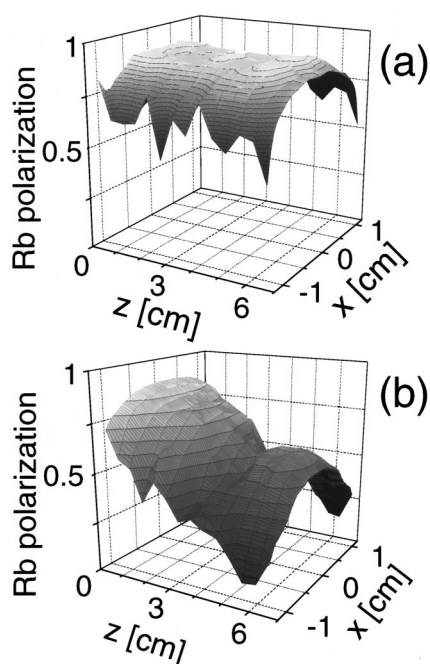


FIG. 3. Two-dimensional absolute polarization image of Rb atoms measured at 50 W of laser power for (a) $T=120$ and (b) 160 °C.

higher than 140 °C the pump laser heats up the front window. Consequently, the Rb density increases near the front window leading to higher absorption of the pumping light and therefore to even stronger heating and so on. Finally, all the pumping light is absorbed a few millimeters after the front window of the cell and $\langle P \rangle$ decreases dramatically. This suggests that for an operating mode requiring lengthy times and higher temperatures, a narrow band pump laser with lower power would prevent the self-induced heating effect and would be more appropriate for a Rb-Xe polarizer. Because of this problem with heating, every measured point shown in this article has been done with only 20 s of optical pumping, and then blocking the pump laser beam for several minutes. For a more detailed picture we independently measured two-dimensional x - z slices of the absolute Rb polarization. Figures 3(a) and 3(b) show two examples of a two-dimensional gradient image measured for a pump laser power of 50 W. The applied magnetic field gradient was $G_x = 0.2$ G/cm. For $T = 120$ °C [Fig. 3(a)] the absolute polarization is almost uniform in the z direction and along the x direction drops by about 25% at the walls of the cell. From this measurement we calculated the volume averaged polar-

ization $\langle P \rangle = 82\%$, which is about 7% higher than in Fig. 2(a). For $T = 160$ °C [Fig. 3(b)] $\langle P \rangle = 53\%$ compared to 49% in Fig. 2(c). For our experimental conditions of nearly homogeneous illumination, all measured volume-averaged polarizations with and without applied gradients differ by less than 10%. Note the local minimum of P at $z = 4$ cm in Fig. 3(b), which appears also in the measurements without gradient in Fig. 2 (triangles). This minimum occurs exactly over the Rb droplet, which is located at $z = 4$ cm on the bottom of the cell. We believe that enhanced evaporation locally over the Rb droplet causes this effect.

In conclusion, we have shown, theoretically and experimentally, how the light of a broadband high power laser penetrates into a high-density Rb vapor. The measured values of the absolute Rb polarization as well as the local optical pumping rates are in approximate agreement with a model, which is based on the crucial parameters of optical pumping under high pressure conditions. Assuming that in the future narrow band diode laser arrays with lower power will be developed, and thereby helping to avoid heating effects, grams of Xe ice with polarization fractions larger than 50% could be produced in the minute regime.

- ¹M. S. Albert, G. D. Cates, B. Driehuys, W. Happer, B. Saam, C. S. Springer, and A. Wishnia, *Nature* (London) **370**, 188 (1994).
- ²M. Ebert, T. Großman, W. Heil, E. Otten, R. Surkau, M. Leduc, P. Bachert, N. V. Knopp, R. Schad, and M. Thelen, *Lancet* **347**, 1297 (1996).
- ³M. E. Wagshul, T. M. Button, H. F. Li, Z. Liang, K. Zhong, and A. Wishnia, *Magn. Reson. Med.* **36**, 183 (1996).
- ⁴J. P. Mugler III, B. Driehuys, J. R. Brookeman, G. D. Cates, S. S. Berr, R. G. Bryant, T. M. Daniel, E. E. de Lange, J. H. Downs III, C. J. Erickson, W. Happer, D. P. Hinton, N. F. Kassel, T. Maier, C. D. Phillips, B. T. Saam, K. L. Sauer, and M. E. Wagshul, *Magn. Reson. Med.* **37**, 809 (1997).
- ⁵G. Navon, Y.-Q. Song, T. Rööf, S. Appelt, R. E. Taylor, and A. Pines, *Science* **271**, 1848 (1996).
- ⁶T. Rööf, S. Appelt, R. Seydoux, E. L. Hahn, and A. Pines, *Phys. Rev. B* **55**, 11604 (1997).
- ⁷A. Bifone, J. Wolber, N. J. Shah, *Il Nuovo Cimento* (in press).
- ⁸B. Driehuys, G. D. Cates, E. Miron, K. Sauer, D. K. Walter, and W. Happer, *Appl. Phys. Lett.* **69**, 1668 (1996).
- ⁹A. Ben-Amar Baranga, S. Appelt, A. R. Young, and W. Happer, *Phys. Rev. A* **58**, 2282 (1998).
- ¹⁰A. R. Young, S. Appelt, A. Ben-Amar Baranga, C. Erickson, and W. Happer, *Appl. Phys. Lett.* **70**, 3081 (1997).
- ¹¹S. Appelt, A. Ben-Amar Baranga, C. J. Erickson, M. V. Romalis, A. R. Young, and W. Happer, *Phys. Rev. A* **58**, 1412 (1998).
- ¹²T. G. Walker and W. Happer, *Rev. Mod. Phys.* **69**, 629 (1997).
- ¹³S. Appelt, A. Ben-Amar Baranga, A. R. Young, and W. Happer, *Phys. Rev. A* **59**, 2078 (1999).
- ¹⁴T. J. Killian, *Phys. Rev.* **27**, 578 (1926).